

Journal of Visualized Experiments

Closed-Cell Gas Reactions In Situ Electron Microscopy

--Manuscript Draft--

Article Type:	Invited Methods Collection - JoVE Produced Video
Manuscript Number:	JoVE62174R3
Full Title:	Closed-Cell Gas Reactions In Situ Electron Microscopy
Corresponding Author:	Kinga Unocic ORNL Oak Ridge, TN UNITED STATES
Corresponding Author's Institution:	ORNL
Corresponding Author E-Mail:	unocicka@ornl.gov
Order of Authors:	Kinga Unocic Dale Hensley Franklin Walden Wilbur Bigelow Michael Griffin Susan Habas Raymond Unocic Lawrence Allard
Additional Information:	
Question	Response
Please indicate whether this article will be Standard Access or Open Access.	Standard Access (US\$2,400)
Please indicate the city, state/province, and country where this article will be filmed . Please do not use abbreviations.	1 Bethel Valley Rd, Oak Ridge, TN 37831
Please confirm that you have read and agree to the terms and conditions of the author license agreement that applies below:	I agree to the Author License Agreement
Please specify the section of the submitted manuscript.	Environment
Please indicate whether this article will be Standard Access or Open Access.	Standard Access (\$1400)
Please provide any comments to the journal here.	

TITLE:

Closed-Cell Gas Reactions *In Situ* Electron Microscopy

AUTHORS AND AFFILIATIONS:

Kinga A. Unocic¹, Dale K. Hensley¹, Franklin S. Walden², Wilbur C. Bigelow³, Michael B. Griffin⁴, Susan E. Habas⁴, Raymond R. Unocic¹, Lawrence F. Allard⁵

¹Center for Nanophase Materials Sciences, Oak Ridge National Laboratory, Oak Ridge, TN, USA.

²Protochips Inc., Morrisville NC, USA.

³Department of Materials Science & Engineering, University of Michigan, Ann Arbor, MI, USA.

⁴National Bioenergy Center, National Renewable Energy Laboratory, Golden, CO, USA.

⁵Materials Science & Technology Division, Oak Ridge National Laboratory, Oak Ridge, TN, USA.

Corresponding Author:

Kinga A. Unocic (unocicka@ornl.gov)

Email Addresses of Co-authors:

Dale K. Hensley (hensleydk@ornl.gov)

Franklin S. Walden (Stamp@protochips.com)

Wilbur C. Bigelow (bigelow@umich.edu)

Michael B. Griffin (Michael.Griffin@nrel.gov)

Susan E. Habas (Susan.Habas@nrel.gov)

Raymond R. Unocic (unocicrr@ornl.gov)

Lawrence F. Allard (allardlfjr@ornl.gov)

Kinga A. Unocic (unocicka@ornl.gov)

KEYWORDS:

in situ reaction, scanning transmission electron microscopy, closed-cell gas reaction, CCGR, gas flow, water vapor, residual gas analyzer, mass spectra, structural materials, catalysis, Pt/TiO₂

SUMMARY:

Here, we present a protocol for performing *in situ* TEM closed-cell gas reaction experiments while detailing several commonly used sample preparation methods.

ABSTRACT:

Gas reactions studied by *in situ* electron microscopy can be used to capture the real-time morphological and microchemical transformations of materials at length scales down to the atomic level. *In situ* closed-cell gas reaction (CCGR) studies performed using (scanning) transmission electron microscopy (STEM) can separate and identify localized dynamic reactions, which are extremely challenging using other characterization techniques. For these experiments, we used a CCGR holder that utilizes microelectromechanical systems (MEMS)-based heating microchips (hereafter referred to as “E-chips”). The experimental protocol described here details

the method for performing *in situ* gas reactions in dry and wet gases in an aberration-corrected STEM. This method finds relevance in many different materials systems, such as catalysis and high-temperature oxidation of structural materials at atmospheric pressure and in the presence of various gases with or without water vapor. Here, several sample preparation methods are described for various material form factors. During the reaction, mass spectra obtained with a residual gas analyzer (RGA) system with and without water vapor further validates gas exposure conditions during reactions. Integrating an RGA with an *in situ* CCGR-STEM system can, therefore, provide critical insight to correlate gas composition with the dynamic surface evolution of materials during reactions. *In situ/operando* studies using this approach allows for the detailed investigation of the fundamental reaction mechanisms and kinetics that occur at specific environmental conditions (time, temperature, gas, pressure), in real-time, and at high spatial resolution.

INTRODUCTION:

There is a need to obtain detailed information on how a material undergoes structural and chemical changes under reactive gas exposure and at elevated temperatures. *In situ* closed-cell gas reaction (CCGR) scanning transmission electron microscopy (STEM) was developed specifically to study the dynamic changes occurring in a wide range of material systems (e.g., catalysts, structural materials, carbon nanotubes, etc.) when subjected to elevated temperatures, different gaseous environments, and pressures from vacuum to full atmospheric pressure^{1-11,12}. This approach can be beneficial in several cases, such as in the accelerated development of new-generation catalysts that are important for a number of industrial conversion processes, such as the single-step conversion of ethanol to n-butenes over Ag-ZrO₂/SiO₂¹³, catalysts for the oxygen reduction reaction, and hydrogen evolution reaction in fuel cell applications^{14,15}, catalytic CO₂ hydrogenation¹⁶, methanol dehydrogenation to formaldehyde or dehydration to dimethyl ether that use either metal catalysts or multi-walled carbon nanotubes in a methanol conversion reaction in the presence of oxygen¹⁷. Recent applications of this *in situ* technique for catalysis research^{1,2,7,8,10-12,18-22} have provided new insight into catalyst dynamic shape changes^{10,11,23}, faceting⁷, growth, and mobility^{8,20,24}. Moreover, *in situ* CCGR-STEM can be used to investigate the high-temperature oxidation behavior of structural materials that are exposed to aggressive environments, from gas turbine engines to next-generation fission and fusion reactors, where not only strength, fracture toughness, weldability, or radiation are important but also high-temperature oxidation resistance²⁵⁻²⁹. Specific to structural alloys, *in situ* CCGR-STEM experiments allow for dynamic tracking of diffusion-induced grain boundary migration under reducing conditions⁹ and measurements of oxidation kinetics at high temperature^{5,6,30}. For several decades prior to the recent development of CCGR technologies, *in situ* gas reaction studies were conducted using dedicated environmental TEMs (E-TEMs). A detailed comparison of E-TEM and CCGR-STEM has been previously addressed¹⁰; therefore, E-TEM capabilities are not discussed further in the present work.

In this work, a commercially available system (**Table of Materials**) comprising of a computer-controlled manifold (gas delivery system) and a specially designed CCGR TEM holder that utilizes a pair of microelectromechanical (MEMS)-based silicon microchip devices (e.g., spacer chip and “E-chip” heater (**Table of Materials**)) were used. Each microchip supports an amorphous,

electron transparent Si_xN_y membrane. The spacer chip has a 50 nm thick Si_xN_y membrane with a 300 x 300 μm^2 viewing area and 5 μm thick epoxy-based photoresist (SU-8) “spacer” contacts that are microfabricated to provide a gas flow path and maintain a physical offset between the two paired microchips (**Figure 1A**). A portion of the E-chip is covered with a low conductivity ~ 100 nm SiC ceramic membrane; the membrane has a 3 x 2 array of 8 μm -diameter etched holes overlapped by a ~ 30 nm thick amorphous Si_xN_y membrane (Si_xN_y viewing area) (**Figure 1A** and **Figure 2D**), through which images are recorded. The E-chip serves a dual role as both specimen support and heater⁶. Au contacts are microfabricated onto the E-chip to allow for resistive heating of the SiC membrane. Each E-chip is calibrated using infrared radiation (IR) imaging methods (**Table of Materials**)² and has been shown to be accurate to within $\pm 5\%$ ³¹. Temperature calibration is independent of the gas composition and pressure, thereby providing independent control over reaction temperatures under any chosen gas conditions. The benefit of a thin-film heater is that temperatures up to 1,000 °C can be reached within milliseconds. In order to perform the reaction, the E-chip is placed on the top of the spacer chip, creating the closed-cell “sandwich” that isolates the environment around the specimen from the high vacuum of the TEM column. The advantage of this setup is that reactions can be performed from low pressures up to atmospheric pressure (760 Torr) with single or mixed gases and under static or flow conditions. The MEMS devices are secured with a clamp (**Figure 1B**) that allows the holder to be inserted within the mm-sized gap of the objective lens pole piece in an aberration-corrected S/TEM instrument (**Table of Materials**) (**Figure 1C**). Modern *in situ* S/TEM holders include integrated micro-fluidic tubing (capillaries) that are connected to the external stainless-steel tubing, which in turn is connected to the gas delivery system (manifold). An electronic control system permits the controlled delivery and flow of reactant gas through the gas cell. Gas flow and temperature are operated by a custom workflow-based software package provided by the manufacturer (**Table of Materials**)^{10,32}. The software controls three gas input lines, two internal experimental-gas delivery tanks, and a receiving tank for gas flow returning from the cell during the experiment (**Figure 1D**).

Due to the variability of materials and their form factor, we first focus on several specimen deposition methods on the E-chip, then outline protocols for performing quantitative *in situ/operando* experiments with controlled temperature, gas mixing and flow.

PROTOCOL

1. E-chip preparation

1.1. Direct powder deposition by drop-casting from a colloidal solution (**Figure 2A**).

1.1.1. Crush the powder if the powder particle aggregates are too large. Do this using a small mortar and pestle (crushed aggregates should be $< 5,000$ nm in size). Mix a small amount (e.g., ~ 0.005 mg, amount determined by experience) of powder in 2 mL of the solvent (e.g., isopropanol or ethanol).

1.1.2. Sonicate the mixture for around 5 min to create a colloidal suspension.

131
132 1.1.3. Place the E-chip on the E-chip retaining fixture. Drop cast approximately 1 μL of the
133 suspension using a 0.5-2.5 μL micro-pipette directly onto the E-chip.

134
135 1.1.4. Clean the Au contacts to remove the suspension with an absorbent paper point while
136 viewing through a stereo microscope.

137
138 1.2. Direct powder deposition through a mask (**Figure 2B**).

139
140 1.2.1. Crush the powder (e.g., Pt/TiO₂) dry, if powder particles are too large (as in 1.1.1).

141
142 1.2.2. Place a new clean E-chip on the E-chip retaining fixture (**Figure 3D**). Use a mask, which is
143 another E-chip with the Si_xN_y membrane removed (by breaking it with tweezers or compressed
144 gas) and place it directly onto the E-chip within the fixture.

145
146 1.2.3. Use the top plate to clamp a new clean E-chip and a mask together within the fixture.

147
148 1.2.4. Deposit a small amount of the powder using a spatula directly on the silicon nitrile
149 membrane in the mask.

150
151 1.2.5. Gently vibrate the fixture to shake the particles down to the E-chip. This can either be
152 done using a vacuum tweezer unit by holding the fixture to the top of the unit while it is running
153 or using a sonication unit and placing the fixture in a dry beaker.

154
155 1.2.6. Shake off the excess powder, disassemble the system and inspect the placement of dry
156 powder on the E-chip using a stereo microscope.

157
158 1.3. Deposition method by either electron beam evaporation, ion, or magnetron sputtering.

159
160 NOTE: This method is used to create either a single-element system or model alloy specimens of
161 known geometry and composition.

162
163 1.3.1. Create a pattern mask (**Figure 3**).

164
165 NOTE: Prepare the pattern mask in advance since it takes some time.

166
167 1.3.2. Use a spacer chip with removed Si_xN_y membrane. In this experiment, a E-chip commonly
168 used in liquid-cell experiments was used after gently breaking out the Si_xN_y membrane which
169 resulted in 50 x 250 μm opening. This spacer chip with removed Si_xN_y membrane will be
170 combined with another chip, having an array of holes (e.g., silicon nitride (SiN) Microporous TEM
171 Window³³).

1.3.3. Use cyanoacrylate (CA) glue (**Table of Materials**) to attach the SiN Microporous TEM Window face down (SiN pattern film away from the spacer chip) over the 50 x 250 μm opening following the manufacturer's recommendation (**Figures 3B,C**).

1.3.4. Repeat the procedure to prepare as many pattern masks as needed, depending on the planned experiments.

1.3.5. Place a new clean E-chip on the E-chip fixture (**Figure 3D**).

1.3.6. Place the pattern mask on the E-chip (**Figures 3C,D**).

1.3.7. Cover with the top plate and clamp it (**Figure 3D**).

1.3.8. Use either electron beam evaporation, ion sputtering or magnetron sputtering deposition techniques. These are the recommended methods used to sputter material of interest directly through the pattern mask.

NOTE: It may be important to purge the deposition system to remove residual oxygen prior to the deposition for higher purity material deposits³³.

1.3.9. Disassemble the system and inspect the E-chip with a stereo microscope to ensure good adherence of the deposited material on the E-chip's Si_xN_y membrane.

1.4. Focused ion beam (FIB) milling (**Figure 2C**).

1.4.1. Prepare a standard TEM lamella using the FIB. Use low kV (e.g., 2-5 kV) for the final milling step to remove damage caused by FIB milling at high voltages (30-40 kV).

1.4.2. Place the TEM lamella on the E-chip using standard FIB procedures. Do not damage the Si_xN_y membrane when attaching FIB prepared TEM lamella to the E-chip. See Allard et al.³⁴ and other publications^{30,35,36} for details of the variety of methods using Xe-PFIB and Ga-FIB instruments for lamella preparation.

2. Preparation of the atmosphere (CCGR-TEM) holder

2.1. Download the desired calibration file.

2.2. Measure the resistance of the SiC heater to ensure that it is within the resistance range for that particular E-chip calibration as provided by the CCGR manufacturer.

2.3. Remove the clamp from the CCGR-TEM holder.

2.4. Clean the tip of the CCGR-TEM holder using absorbent paper points and/or compressed air, making sure no debris remains on the O-ring grooves. Then place the special double-gasket seal within the tip.

2.5. Place the spacer chip into the CCGR-TEM holder.

2.6. Place the E-chip containing the specimen that was prepared by one of the methods mentioned in section 1 with the heater contacts down onto the spacer chip, making a proper connection to the electrical contacts of the flex-cable within the holder.

2.7. Position the holder clamp plate on the top of the E-chip using tweezers, place the screws into the designated location at the tip of the CCGR-TEM holder, then torque the set screws with a final torque to 0.2 lb-ft.

2.8. Measure again, the resistance of the SiC heater after assembling the CCGR-TEM holder to ensure that it is within the resistance range for that particular E-chip calibration as provided by the CCGR manufacturer.

NOTE: Here, a special adapter is used, which plugs directly into the holder's electrical connections. This allows for the resistance measurements to be made through the CCGR-TEM holder and paired microchip devices assembly while fully assembled into the holder.

3. Preparation of the experimental setup

3.1. Bake and pump down the system (manifold, holder, gas tanks, and RGA chamber) overnight, either with or without the holder connected by pressing the **Bake** button in the gas-control software.

3.2. Load the holder into the scanning transmission electron microscope and connect the gas tubing from the manifold to the CCGR-TEM holder.

3.3. For the experiment, pump and purge the system with an inert gas (e.g., Ar or N₂) twice from 100 Torr to 0.5 Torr.

3.4. Perform a final pump and purge from 100 Torr to 0.001 Torr. This will ensure that the entire gas delivery system, from the gas manifold to the holder, is cleaned and flushed with inert gas.

3.5. Residual gas analyzer – During the pump and purge procedure, turn on the RGA system to warm up the filament.

4. Preparing the water vapor delivery system (VDS)

NOTE: These instructions are for specific experiments that involve controlled delivery of gas in vapor form (e.g., water vapor). Gas delivery control is through the gas-control software provided by the manufacturer (**Table of Material**).

4.1. Attach the purge gas (e.g., nitrogen) to the VDS, turn the lever knob to **Exhaust**, and then turn to the **Park** position.

4.2. Purge the VDS (repeat 4.1) by flowing inert gas three times or until no more liquid is present.

4.3. Turn the lever knob to the **Park** position and attach the VDS to the manifold.

4.4. Turn the lever knob to the **Fill** position and remove the purge gas line.

4.5. Set the vapor pressure to 18.7 Torr in the gas-control software.

4.6. In the software, pump the VDS to vacuum (0.1 Torr) by selecting the input line and pressing the pump button.

4.7. Fill the VDS with water (2 mL) via a syringe and tubing.

NOTE: If higher purity vapor is needed, additional purging steps may be required.

5. Running the reaction

5.1. Make sure all gases that are to be used in the experiments (e.g., nitrogen, water vapor, and oxygen) are connected to the manifold.

5.2. With the gas-control software under **Naming**, set the name(s) for the gas(es) required for the reaction and save the raw “.csv” file such that a running log file is generated for the experiment.

5.3. Under the **E-chip Setup**, select the associated calibration file (i.e., as described in 2.5) for the E-chip being used and **Run Calibration**. As previously mentioned in the introduction section, each E-chip is temperature calibrated using infrared radiation (IR) imaging from the manufacturer.

5.4. Under **Pump and Purge**, see **Preparation of Experimental Setup**.

5.5. Under **Gas Control**, select the desired gas name and its composition (e.g., select percentage for each gas) for the experiment.

5.6. Under **Temperature**, select the desired heating rate and target temperature for the temperature of interest for the experiment and press the **Start** button.

5.7. Start flowing the gas by pressing the **Start** button under the **Gas Control** section.

6. End of the experiment

6.1. Once the reaction is complete, stop flowing the gas, turn off the temperature knob, and end the session using the **Pump** and **Purge** procedure (e.g., depending on the reaction that was performed, perform **Pump** and **Purge** procedure from 100 Torr to 0.1 Torr 2-3 times).

6.2. Prior to removing the *in situ* CCGR-TEM holder from the electron microscope, ensure that that holder pressure is brought back up to atmospheric pressure.

REPRESENTATIVE RESULTS

Specimens for MEMS-Based Closed-Cell Gas Reactions:

Direct powder deposition by drop casting from a colloidal solution and through a mask

Depending on the material to be studied, there are a number of different ways to prepare E-chips for *in situ/operando* CCGR-STEM experiments. Preparing the gas cell for catalysis studies typically requires dispersion of the catalyst nanoparticles onto the E-chip of the material either from a colloidal liquid suspension (**Figure 2A**), or directly from the dry powder itself (**Figure 2B**). For coarser powders, it may be necessary to crush the particle size (e.g., using a mortar and pestle or by placing the powder between glass slides), so the powder aggregates will fit within the 5 μm gap between paired microchips (“sandwich”) size without damaging the Si_xN_y membranes. When using a liquid suspension, the deposition of powders results in wider dispersion covering a larger area of the E-chip, which often requires a secondary cleaning (“dusting”) step to remove the powder from the gold contacts. Whereas, when depositing dry powder, a *mask* can be used to directly deposit powder in the desired location (e.g., the electron-transparent Si_xN_y viewing area). In our study, the masks we tested are E-chips with removed Si_xN_y membrane and liquid-cell spacer chip with removed Si_xN_y film. Since the latter one has a narrower opening (50 x 250 μm), a more precise deposition can be achieved directly onto the membrane heater region of the E-chip, and no additional cleaning of the gold contacts is necessary.

Pattern mask and alloy deposition

Deposition of the catalyst on the E-chip is relatively easy when compared with bulk alloys. Since nano-sized particles of random alloy compositions are not readily available and crushing alloy micro-size powders has also been problematic⁶, the evaluation of one more potential new method was addressed for producing alloy specimens of controlled composition and geometry onto gas-cell E-chip membranes³³.

The basic idea for the structural alloy specimens is to deposit “islands” (**Figure 2D**) of the desired structural material using a suitable vapor deposition technique (e.g., electron beam evaporation, ion sputtering, or magnetron sputtering) where the elemental species are deposited directly onto the E-chip membrane (**Figure 3A**) through a *pattern mask* composed of an array of $\sim 2\ \mu\text{m}$ diameter holes (**Figure 3**). The *pattern mask* can be produced by FIB-milling techniques, using a Si_xN_y spacer E-chip. Alternatively, it is easier to use a commercially available 50 nm thick SiN

Microporous TEM Window, with an array of 2 μm pores in a silicon nitride film in a grid pattern within a single 500 x 500 μm membrane (**Table of Materials**)³³ as a *pattern mask* (**Figure 3B-b**). As shown, it is possible to attach a SiN Microporous TEM Window to an E-chip with removed Si_xN_y membrane (**Figure 3B-a**) and place it directly on the E-chip (**Figure 3C**) in a securely tightened E-chip fixture (**Figure 3D**). This is used to create a perfect alignment of the devices and helps isolate the evaporated species to a small area on the E-chip (**Figure 3C-c and 3C-d**). Depending on the chemical composition of the depositing alloy/material, each evaporation technique (electron beam evaporation, ion sputtering, or electron magnetron sputtering) has its own advantages and disadvantages³³, which will not be addressed here. Therefore, the idea for gas-reactor sample preparation by the vapor-phase deposition through a *pattern mask* onto the E-chip surface has potential for further development and experimentation.

FIB milling

E-chip preparation becomes more challenging when investigating solid materials. Comparable studies of bulk structural materials require preparation of the sample as a thin slice or lamella of suitable specimen thickness and geometry (e.g., electron transparent, and a few microns in lateral extent) that can be secured in some fashion to the E-chip membrane. This process can be conducted using FIB-milling procedures and placing the TEM lamella on the Si_xN_y viewing area in the SiC heater membrane (**Figure 2C-c**)^{9,30,36,37} with the caveat that conventional gallium FIB milling typically leaves residual Ga, either as Ga implantation and/or Ga segregation in some material systems (e.g., within grain boundaries and phases in Al and its alloys³⁸) on the milled surface, thereby complicating the reaction process when dynamic events need to be examined at the atomic level. It is essential to evaluate material susceptibility to Ga penetration⁹. To minimize Ga implantation and surface damage, we can use electropolished needles, similar to the ones used for atom probe tomography, which can then be placed on the E-chip (**Figure 2C-d**) using the FIB by attaching the sample by W or Pt “tack” points³¹. EDS analysis confirms that Ga implantation can be decreased/eliminated (**Figure 2C-d**; however, the limitation of this method is the geometry of the sample. Only needle-shaped samples can be prepared without exposing the area of interest to Ga ions. As an alternative, new Xe-plasma FIBs can be used to prepare thin lamella without Ga implantation. For example, electron-transparent lamella from 3-mm electropolished discs can be extracted and placed on the E-chip (**Figure 2C-e**) resulting in a large area of the sample with no issues associated with a residual ion implantation layer (Xe is inert and does not tend to deposit on sample surfaces. It also produces a thinner amorphous layer (~1 nm) than the best FIB procedures with Ga source)³⁴.

In situ reaction experiments

In order to capture dynamic events, first, it is necessary to bake and pump down the system overnight. During the actual experiment, the holder is connected to the gas manifold system and is pumped and purged several times. The system is initially pumped down twice from 100 Torr to 0.5 Torr and purged with an inert gas (e.g., N_2 , Ar); the third cycle involves pumping down to 0.001 Torr. The internal conditions are monitored by an RGA system (**Table of Materials**), which is equipped with an electron multiplier¹⁰. The RGA is integrated into the gas-control system through connection to the return side of the CCGR-TEM holder (**Figure 4B**). To remove residual water vapor and other gases from the RGA chamber, heating tape is used which permits for bake-

outs between experiments. An ultra-high vacuum in the RGA of $< 2 \times 10^{-8}$ Torr can be achieved. An electronically controlled leak valve (LV) is used to control the amount of gas from the holder and into the RGA chamber, and a return capillary line to the manifold is isolated from the leak valve with a hand valve (HV).

An example of the recorded gas partial pressures measured in the RGA chamber, CCGR-TEM holder (LV open), manifold (H1 open), and Tank 1 (T1 open) before *in situ* experiments are shown in **Figure 4**. This demonstrates that even though overnight baking, pumping down and purging were performed, there is still some degree of residual water vapor. Thus, for experiments particularly with water vapor, it is important to establish the baseline for initial conditions of the system and record the initial partial pressures. For our system shown in **Figure 4**, the partial pressure of water vapor measured all the way to Tank 1 reads 1.1×10^{-7} Torr. The atomic mass spectrum versus partial pressure shows the water vapor peak at 18 amu, reaching 1.1×10^{-7} Torr (**Figure 3C**). Comparing the spectrum with the one from the experiments that contained O_2 and water vapor, there is a significant increase in the partial pressure (2.5×10^{-7} Torr) of the peak at 18 amu. Note that by further opening the leak valve, more gas flow is introduced into RGA chamber where measurements are performed. It is important to adjust the leak valve in such a way that the total pressure of the experiment is kept constant in order to compare results between conditions. Gas composition measurements are possible when the RGA chamber pressure is in the $\leq 10^{-5}$ Torr range, which is less than a billionth of an atmosphere due to the high reactivity of ions and their short life; therefore, the pressures in the RGA are much lower than within the gas cell.

The attachment of the water vapor delivery system to the manifold requires purging the VDS with inert gas until no liquid is present (it is also important to clean the VDS right after the experiment to make this step simpler) and keep it purged during the connection to the manifold. Before the VDS is filled with the desired liquid (e.g., water, methanol, or ethanol), first, the VDS is pumped down to vacuum. Then, the liquid is added using a syringe and tubing. To improve the quality of the vapor, with reduced oxygen content) the experimental supply tank can be filled with the vapor and pumped down two or three times; otherwise, it is ready to be used.

The gas-control software guides the user through the settings during all phases of the experiment. In the beginning, the correct gases and pressures need to be selected. The resistance of the E-chip must be checked to ensure that the E-chip was not damaged during loading into the CCGR-TEM holder. In the manifold, there are two supply tanks (Tank 1 and Tank 2) that hold and supply gas with a final composition for the reaction. The desired gas composition can be obtained by mixing the media directly in one of the supply tanks (Tank 1 or Tank 2 in **Figure 1D** and **4B**). The manifold system has three ports that introduce gases to the manifold. However, if more than three gases are desired to be mixed, one or more of the input lines need to be split. Alternatively, if the gas composition is very complicated, pre-mixed gases should be used, which allows their mixing during the experiment with the desired vapor composition.

After setting the desired gas composition for the *in situ* experiment, the gas-control software will first introduce the lower percentage gas; then after reaching the desired pressure, it will feed the

second gas into the supply tank. Afterward, depending on the experiment, the introduction of the gas into the gas cell can be either at room temperature or after heating the sample to the desired temperature at a certain/desired heating rate. This depends on each user's experiment. The heating can be in a vacuum, under inert gas, or under the premixed gas that will be used in the experiments. When the gas needs to be changed while running experiments, the system is pumped down and purged with inert gas to avoid any hazard of mixing two undesired gases.

In general, there is little or no drift in the x and y directions during the experiments, but during heating and/or pressure changes, significant variation in the specimen height is observed (which poses a challenge to capture the initiation of a reaction). If possible, heat to the desired temperature under vacuum or inert gas, adjust all the alignments and then introduce the gas media. Experiments below 200 °C are also challenging with the closed-cell due to contamination build up on the surface of the microchip viewing area.

As an example, the evolution of the surface of Pt nanoparticles on TiO₂ support was captured when exposed to 100% water vapor at 17 Torr at 300 °C (**Figure 5**). The structural changes in the Pt particle and rearrangement of the structure to expose {111} surfaces (**Figure 6**) were observed (**Figure 6A vs. Figure 6B vs. Figure 6C**).

FIGURE LEGENDS

Figure 1: E-chip paired device with CCGR-TEM holder. (A) Pair of MEMS-based silicon microchip devices (spacer chip and E-chip (heater)) for *in situ* CCGR-STEM experiments. (B) Schematic of the CCGR-TEM holder tip with paired microchip devices being secured with a clamp. (C) Cross-section of the CCGR-TEM holder tip showing E-chip placed on top of the spacer chip creating the closed-cell (sandwich) that isolates environment around the specimen from TEM column. (D) Closer view of manifold that encloses three gas input lines on the side, two experimental gas delivery tanks, and a receiving tank for gas flow control during the experiment. (Images provided by the CCGR system manufacturer).

Figure 2: Example of different deposition techniques for preparing samples on the E-chip. (A) E-chip with catalyst deposited by drop-casting from a colloidal solution. (B) E-chip after dry powder deposition using two different masks (a) E-chip with removed Si_xN_y membrane and (b) liquid-cell E-chip with removed Si_xN_y membrane. (C) E-chip prepared by (a) standard FIB-milling procedures and placement of FIB lamella on Si_xN_y electron transparent viewing areas, (b) electropolished needles, (c) 3 mm electropolished discs extracted by plasma FIB and placed on E-chip. (D) Higher magnification image of E-chip with alloy deposited through *pattern mask*.

Figure 3: E-chip preparation using sputtering techniques. (A) Schematic of the E-chip. (B) *Pattern mask* fabricated from liquid-cell E-chip with Si_xN_y membrane removed and 50 nm thick SiN Microporous TEM Window (B-a), with arrays of 2 μm pores in silicon nitride film in a grid pattern within single 500 x 500 μm membrane window³⁴ that overlaps the 50 x 250 micron opening of the liquid-cell microchip (B-b). (C) *Pattern mask* directly placed on the E-chip (C-c) with higher magnification image showing the alignment of Si_xN_y viewing area with 50 x 250 μm opening in liquid-cell E-chip that is covered with SiN Microporous TEM Window (3C-d and also 3B-b). (D) E-

chip cross-section within the fixture (**D-e**), top view (**D-g**), and (**D-f**) closeup view of the *pattern mask* in the E-chip fixture. E-chip fixture holds *pattern mask* placed on E-chip in secure manner during vapor-phase deposition.

Figure 4: Measuring gas compositions using a residual gas analyzer. (**A**) Example of gas partial pressures measured in RGA chamber, CCGR-TEM holder (LV open), manifold (H1 open), and Tank 1 (T1 open) before *in situ* experiments. (**B**) Schematic of the gas-control software showing locations for RGA measurements before experiments. (**C**) Mass spectra generated in a vacuum before the experiment (red) with water vapor peak at 18 amu reaching 1.1×10^{-7} Torr and during the experiment (blue) with a mixture of O_2 with H_2O showing an increase in the partial pressure for OH, H_2O , and O_2 . RGA confirms the presence of H_2O in *in situ* closed-cell.

Figure 5: Measuring water vapor content. (**A**) Schematic of the gas-control software showing an example of 100% water vapor introduced to Tank 1 with test parameters recorded by the gas-control system at room temperature before the experiment. (**B**) Gas partial pressure spectra acquired using the RGA before (red) and during (blue) reaction with 100 % water vapor at 17 Torr and 300 °C.

Figure 6: Experimental results of water vapor exposure effects on Pt nanoparticle structure. (**A-C**) BF-STEM images showing the reconstructed surface of a Pt nanoparticle on TiO_2 support when exposed to 100 % water vapor at 17 Torr and 300 °C.

DISCUSSION

In the present work, an approach to perform *in situ* STEM reactions with and without water vapor is demonstrated. The critical step within the protocol is E-chip preparation and maintaining its integrity during the loading procedure. The limitation of the technique is (a) the specimen size and its geometry to fit the nominal 5- μm gap between paired (MEMS)-based silicon microchip devices as well as (b) a total pressure used in the experiments with water vapor since the highest total pressure depends on the quantity of water vapor⁶. The significance of this method with respect to existing methods is that we can perform *operando* experiments, i.e., we analyze the specimens under real conditions, enabled by an RGA system that confirms/monitors experimental conditions. Additionally, there are opportunities for future applications of the technique to diverse materials systems that may require different methods and procedures for sample deposition on E-chip heaters.

The E-chip preparation is shown in **Figure 2**, which highlights four different sample preparation methods; (1) direct powder deposition by drop cast from colloidal solution, (2) direct powder deposition through *mask*, (3) direct EBID/IBID or magnetron sputtering with *patterned masks* and (4) FIB milling. Powder deposition should include only powders with particles or aggregates less than 5 μm thick to fit within the nominal 5 μm gap between paired microchips in order to prevent damage to the Si_xN_y viewing windows^{2,6}. Researchers performing deposition through evaporation methods should adjust the parameters according to the elemental composition, temperature, and humidity and should minimize the oxygen level. Sample preparation using FIB milling requires users to be extremely careful to prevent damage to the Si_xN_y membrane. Also, Ga

implantation could alter alloy chemistry and affect surface diffusion. Regardless of what E-chip specimen method is selected, following sample deposition, examination of the E-chip using light optical microscopy and resistance measurements are required to verify the E-chip integrity before starting the *in situ* experiments.

This protocol for *in situ* CCGR-STEM studies enables new opportunities to visualize nanoscale gas reactions while they occur and under realistic conditions (temperature, pressure, and gas composition). Now, it is possible to reveal dynamic changes in the surface atoms and interfaces and to understand how the surface composition and structure may be controlled by external means⁷. For example, the structural changes in the Pt particle and rearrangement of its structure to expose {111} surfaces (**Figure 6**) were associated with minor shape changes (**Figure 6A vs. 6B vs. 6C**). Catalytic performance is determined by interfacial reactions that occur at site-specific catalyst interfaces, and *in situ* microscopy helped uncover gas-surface phenomena under water vapor in Pt/TiO₂ catalysis research. Moreover, the experimental protocol presented here also contributes to an improved understanding of the *in situ* gas reaction process by monitoring the gas composition using an RGA. This is important because of the need to correlate the role of gas composition with structural and chemical changes that the material being studied undergoes as a direct effect of environmental exposure.

In summary, *in situ* CCGR-STEM studies can enable capturing the deactivation or regeneration of catalyst materials via imaging and spectroscopy, and the investigation of chemical and morphological changes during gas reactions on bulk alloy materials. Such studies also allow on an identification of the minimum temperature of initiation of e.g., the regeneration reaction and/or the maximum temperature for the reaction, as well as the nature of coarsening of supported metal particles from which kinetic information can be extracted. These studies provide a direct link to current computational models that predict the direction of the reactions, but not time (when it will happen for material optimization). The potential of this environmental closed-cell gas reaction protocol can be expanded to a number of different materials in conjunction with quantitative spectroscopy techniques such as electron energy-loss spectroscopy³⁹ and energy-dispersive X-ray spectroscopy^{5,6} to identify chemical compositions and/or oxidation state changes. Moreover, this is just the beginning of a new capability that creates an advanced opportunity for materials characterization under a variety of realistic conditions.

DISCLOSURE:

The authors declare no conflicts of interest.

This manuscript has been authored by UT-Battelle, LLC under Contract No. DE-AC05-00OR22725 with the U.S. Department of Energy. The United States Government retains and the publisher, by accepting the article for publication, acknowledges that the United States Government retains a non-exclusive, paid-up, irrevocable, worldwide license to publish or reproduce the published form of this manuscript, or allow others to do so, for United States Government purposes. The Department of Energy will provide public access to these results of federally sponsored research in accordance with the DOE Public Access Plan (<http://energy.gov/downloads/doe-public-access-plan>).

ACKNOWLEDGMENTS

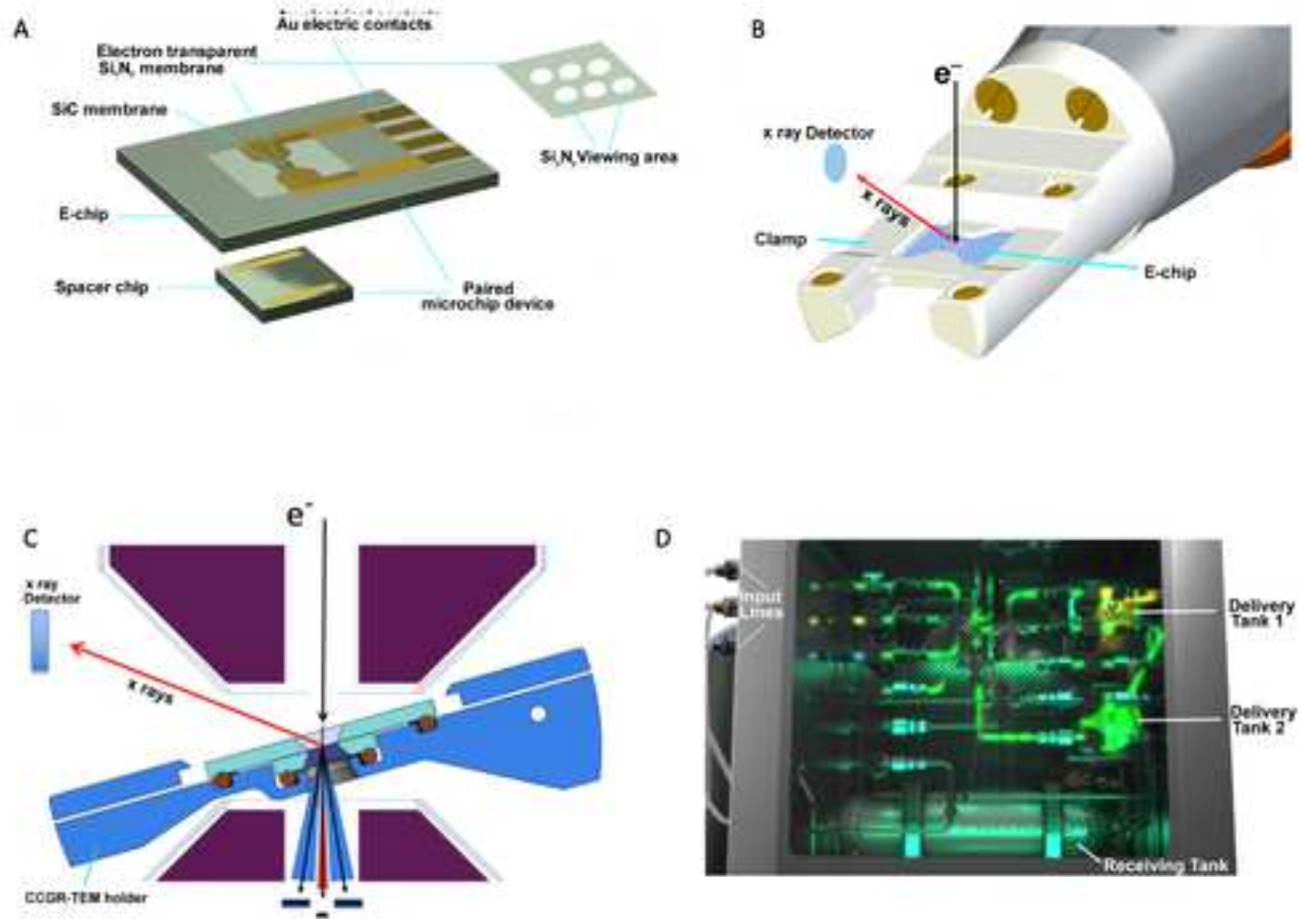
This research was sponsored by the Laboratory Directed Research and Development Program of Oak Ridge National Laboratory, managed by UT-Battelle LLC, for the U.S. Department of Energy. Part of the development to introduce water vapor into the *in situ* gas cell was performed in collaboration with ChemCatBio, a member of the Energy Materials Network, and was supported by the U.S. Department of Energy Bioenergy Technology Office under Contract no DE-AC05-00OR22725 with Oak Ridge National Laboratory. Part of the sample preparation was supported by the Center for Nanophase Materials Sciences (CNMS), which is sponsored by the Scientific User Facilities Division, Office of Basic Energy Sciences, the U.S. Department of Energy. We thank Dr. John Damiano, Protochip Inc., for useful technical discussions. The authors thank Rosemary Walker and Kase Clapp, ORNL production team, for support with movie production.

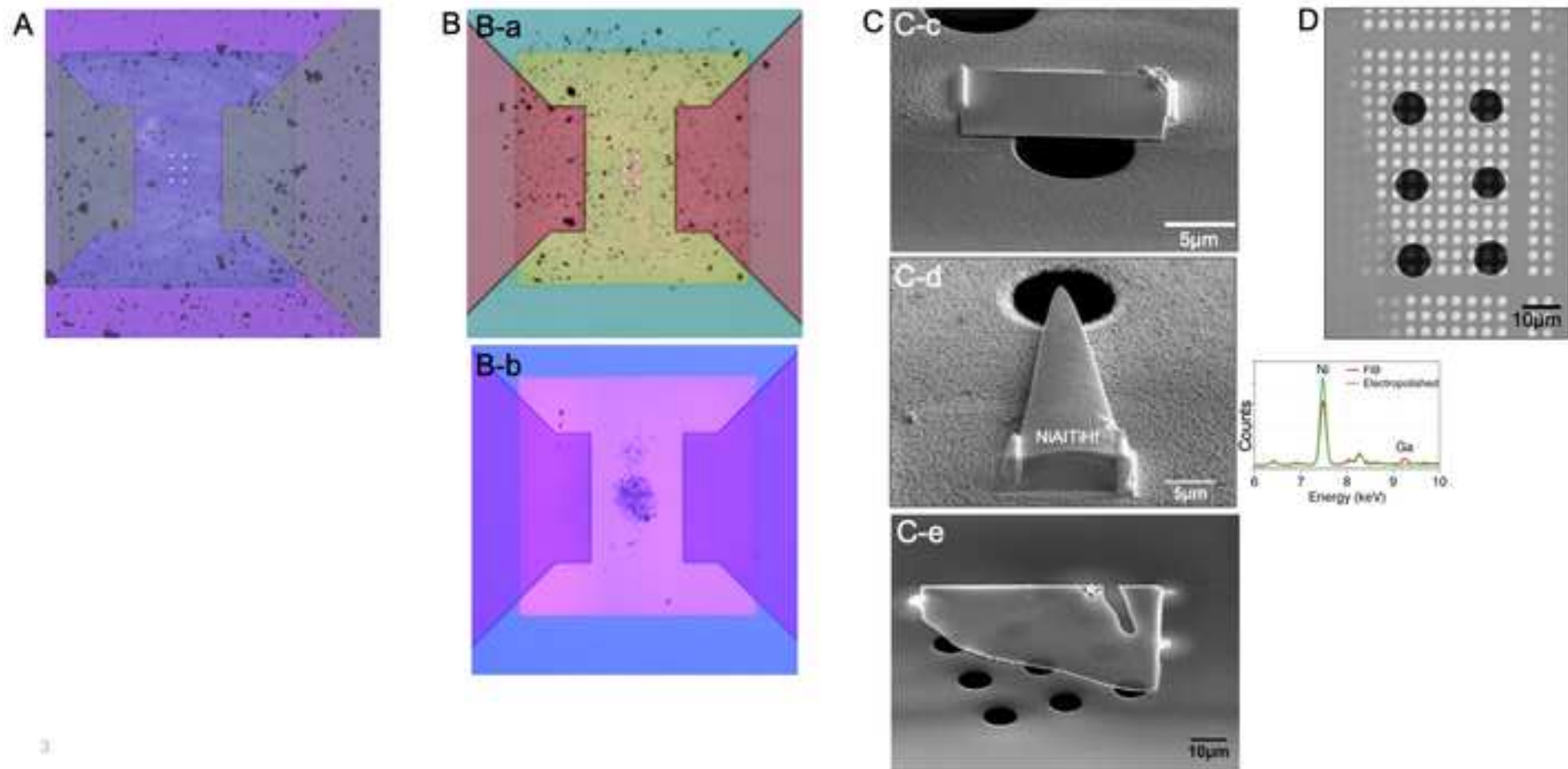
REFERENCES

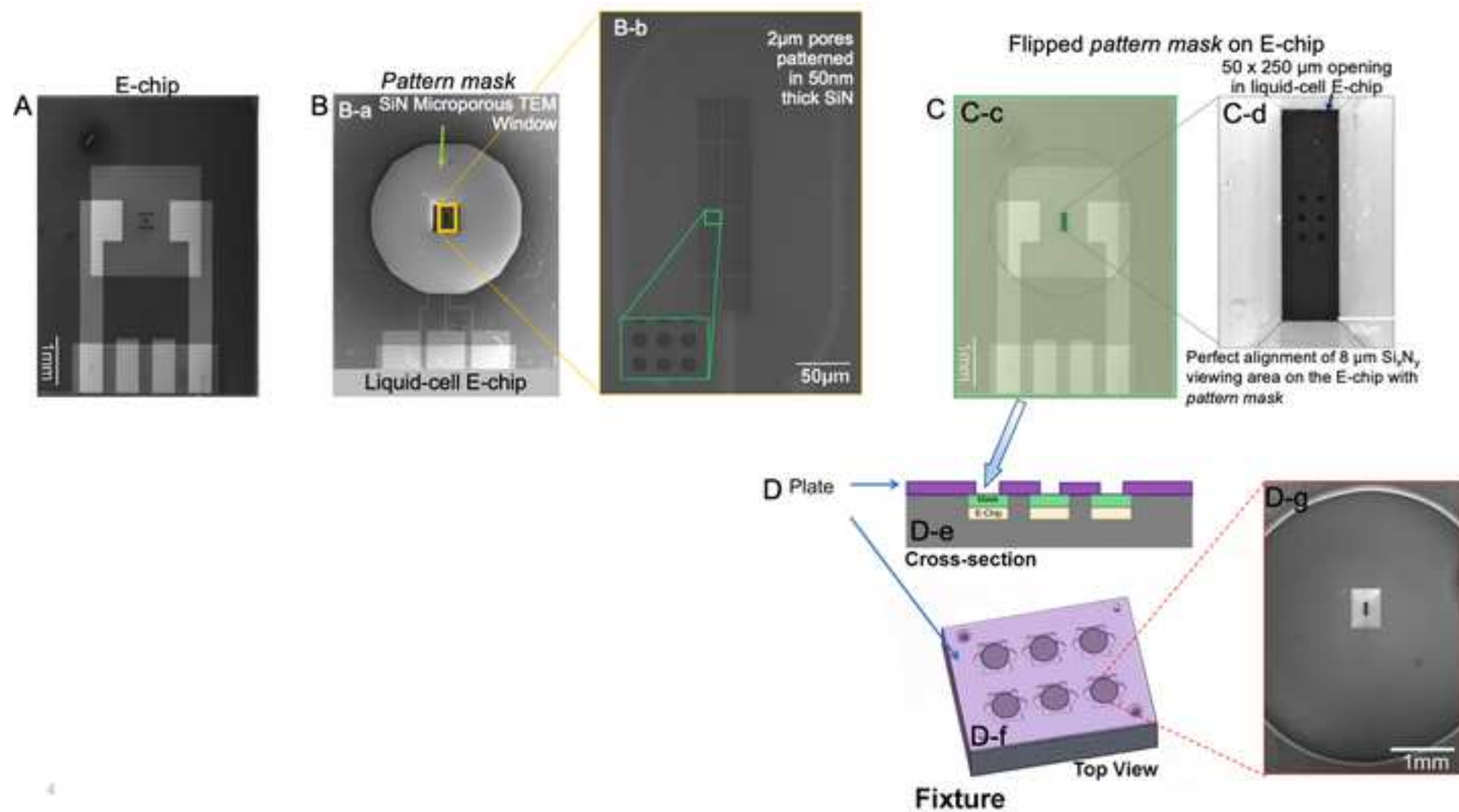
1. Allard, L. F. et al. A new MEMS-based system for ultra-high-resolution imaging at elevated temperatures. *Microscopy Research and Technique*. **72** (3), 208–215 (2009).
2. Allard, L. F. et al. Novel MEMS-based gas-cell/heating specimen holder provides advanced imaging capabilities for *in situ* reaction studies. *Microscopy and Microanalysis*. **18** (4), 656–666 (2012).
3. Allard, L. F. et al. Innovative closed-cell reactor permits *in situ* heating and gas reactions with atomic resolution at atmospheric pressure. *Microscopy and Microanalysis*. **18** (S2), 1118–1119 (2012).
4. Allard, L. F. et al. Controlled *in situ* gas reaction studies of catalysts at high temperature and pressure with atomic resolution. *Microscopy and Microanalysis* **20** (S3), 1572–1573 (2014).
5. Allard, L. F. et al. computer-controlled *in situ* gas reactions via a mems-based closed-cell system. *Microscopy and Microanalysis*. **21** (S3), 97–98 (2015).
6. Unocic, K. A., Shin, D., Unocic, R. R., Allard, L. F. NiAl oxidation reaction processes studied *in situ* using MEMS-based closed-cell gas reaction transmission electron microscopy. *Oxidation of Metals*. **88** (3-4), 495–508 (2017).
7. Dai, S. et al. Revealing surface elemental composition and dynamic processes involved in facet-dependent oxidation of Pt₃Co nanoparticles via *in situ* transmission electron microscopy. *Nano Letters*. **17** (8), 4683–4688 (2017).
8. Dai, S., Zhang, S., Katz, M. B., Graham, G. W., Pan, X. *In Situ* observation of Rh-CaTiO₃ catalysts during reduction and oxidation treatments by transmission electron microscopy. *ACS Catalysis*. **7** (3), 1579–1582 (2017).
9. Burke, M. G., Bertali, G., Prestat, E., Scenini, F., Haigh, S. J. The application of *in situ* analytical transmission electron microscopy to the study of preferential intergranular oxidation in Alloy 600. *Ultramicroscopy*. **176**, 46–51014 (2017).
10. Unocic, K. A. et al. Introducing and controlling water vapor in closed-cell *in situ* electron microscopy gas reactions. *Microscopy and Microanalysis*. **26** (2), 229–239 (2020).
11. Vendelbo, S. B. et al. Visualization of oscillatory behaviour of Pt nanoparticles catalysing CO oxidation. *Nature Materials*. **13** (9), 884–890 (2014).

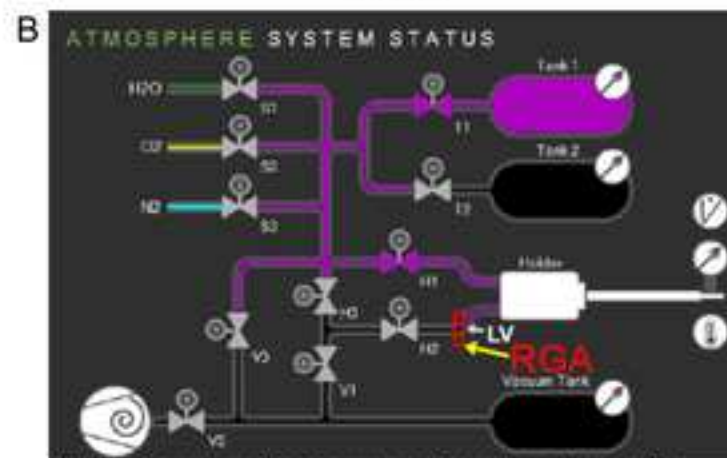
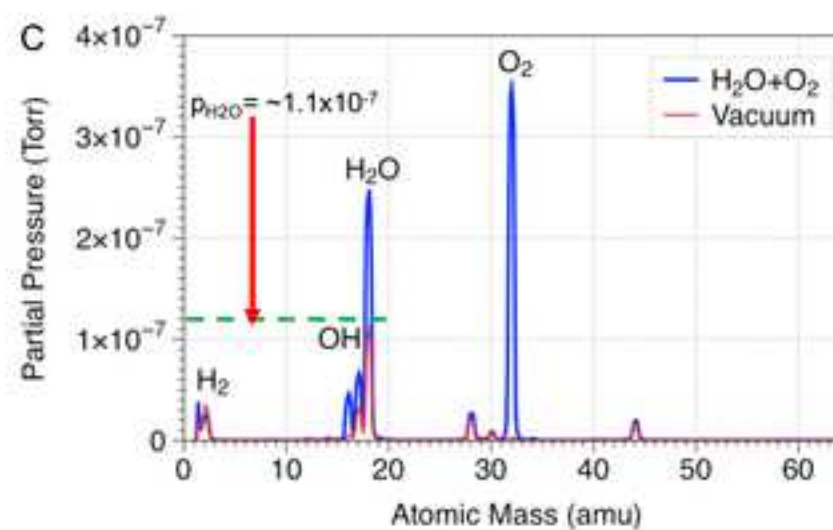
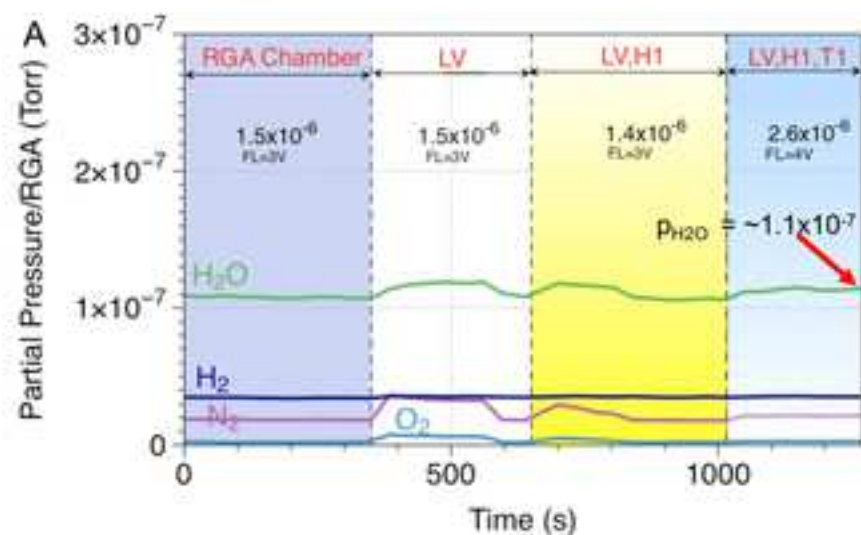
12. Moliner, M. et al. Reversible transformation of Pt nanoparticles into single atoms inside high-silica chabazite zeolite. *Journal of the American Chemical Society*. **138** (48), 15743–15750 (2016).
13. Dagle, V. et al. Single-step conversion of ethanol to n-butenes over Ag-ZrO₂/SiO₂ catalysts. *ACS Catalyst*. **10** (18), 10602–10613 (2020).
14. Chi, M. et al. Surface faceting and elemental diffusion behaviour at atomic scale for alloy nanoparticles during in situ annealing. *Nature Communications*. **6** (1), 1–9 (2015).
15. Zhao, X. et al. Single-iron site catalysts with self-assembled dual-size architecture and hierarchical porosity for proton-exchange membrane fuel cells. *Applied Catalysis B: Environmental*. **279**, 119400 (2020).
16. Baddour, F. G. et al. An Exceptionally mild and scalable solution-phase synthesis of molybdenum carbide nanoparticles for thermocatalytic CO₂ hydrogenation. *Journal of the American Chemical Society*. **142** (2), 1010–1019 (2019).
17. Yan, P. et al. Methanol oxidative dehydrogenation and dehydration on carbon nanotubes: active sites and basic reaction kinetics. *Sustainable Energy Fuels*. **10**, 4952–4959 (2020).
18. Unocic, R. R., Jungjohann, K., Mehdi, B. L., Browning, N. D., Wang, C. *In situ* electrochemical scanning/transmission electron microscopy of electrode–electrolyte interfaces. *MRS Bulletin*. **45**, 1–8 (2020).
19. LaGrow, A. P., Lloyd, D. C., Gai, P. L., Boyes, E. D. *In situ* scanning transmission electron microscopy of Ni nanoparticle redispersion via the reduction of hollow NiO. *Chemistry of Materials*. **30** (1), 197–203 (2017).
20. Liu, L., Zakharov, D. N., Arenal, R., Concepcion, P., Stach, E. A., Corma, A. Evolution and stabilization of subnanometric metal species in confined space by *in situ* TEM. *Nature Communications*. **9** (1), 574 (2018).
21. Wu, Y. A. et al. Visualizing redox dynamics of a single Ag/AgCl heterogeneous nanocatalyst at atomic resolution. *ACS Nano*. **10** (3), 3738–3746 (2016).
22. Li, Y. et al. Complex structural dynamics of nanocatalysts revealed in operando conditions by correlated imaging and spectroscopy probes. *Nature Communications*. **6** (1), 7583 (2015).
23. Hansen, P. L. et al. Atom-resolved imaging of dynamic shape changes in supported copper nanocrystals. *Science* **295** (5562), 2053–2055 (2002).
24. Creemer, J. F. et al. Atomic-scale electron microscopy at ambient pressure. *Progress in Materials Science*. **108**, 993–998 (2008).
25. Was, G. S., Petti, D., Ukai, S., Zinkle, S. Materials for future nuclear energy systems. *Journal of Nuclear Materials*. **527**, 151837 (2019).
26. Unocic, K. A., Yamamoto, Y., Pint, B. A. Effect of Al and Cr content on air and steam oxidation of FeCrAl alloys and commercial APMT alloy. *Oxidation of Metals*. **87** (3–4), 431–441 (2017).
27. Zinkle, S. J. et al. Fusion materials science and technology research opportunities now and during the ITER era. *Fusion Engineering and Design*. **89** (7–8), 1579–1585 (2014).

28. Quadakkers, W. J., Olszewski, T., Piron-Abellan, J., Shemet, V., Singheiser, L. Oxidation of metallic materials in simulated CO₂/H₂O-rich service environments relevant to an oxyfuel plant. *Materials Science Forum*. **696**, 194–199 (2011).
29. Gleeson, B. Thermal barrier coatings for aeroengine applications. *Journal of Propulsion and Power*. **22** (2), 375–383 (2006).
30. Unocic, K. A., Allard, L. F., Coffey, D. W., More, K. L., Unocic, R. R. Novel method for precision controlled heating of TEM thin sections to study reaction processes. *Microscopy and Microanalysis*. **20** (S3), 1628–1629 (2014).
31. Idrobo, J. C. et al. Temperature measurement by a nanoscale electron probe using energy gain and loss spectroscopy. *Physical Review Letters*. **120** (9), 095901 (2018).
32. Unocic, K. A., Datye, A. K., Bigelow, W. C., Allard, L. F. Water vapor in closed-cell *in situ* gas reactions: Initial experiments. *Microscopy and Microanalysis*. **23** (S1), 940–941 (2017).
33. Allard, L. F., Meyer, H. M., Hensley, D. K., Bigelow, W. C., Unocic, K. A. Model “alloy” specimens for MEMS-based closed-cell gas-reactions. *Microscopy and Microanalysis*. **23** (S1), 908–909 (2017).
34. Allard, L. F. et al. The utility of Xe-plasma FIB for preparing aluminum alloy specimens for MEMS-based *in situ* double-tilt heating experiments. *Microscopy and Microanalysis*. **25** (S2), 1442–1443 (2019).
35. Schilling, S., Janssen, A., Zaluzec, N. J., Burke, M. G. Practical aspects of electrochemical corrosion measurements during *in situ* analytical transmission electron microscopy (TEM) of austenitic stainless steel in aqueous media. *Microscopy and Microanalysis*. **23** (4), 741–750 (2017).
36. Zhong, X. L., Schilling, S., Zaluzec, N. J., Burke, M. G. Sample preparation methodologies for *in situ* liquid and gaseous cell analytical transmission electron microscopy of electropolished specimens. *Microscopy and Microanalysis*. **22** (6), 1350–1359 (2016).
37. Duchamp, M., Xu, Q., Dunin-Borkowski, R. E. Convenient preparation of high-quality specimens for annealing experiments in the transmission electron microscope. *Microscopy and Microanalysis*. **20** (6), 1638–1645 (2014).
38. Unocic, K. A., Mills, M. J., Daehn, G. S. Effect of gallium focused ion beam milling on preparation of aluminum thin foils. *Journal of Microscopy*. **240** (3), 227–238 (2010).
39. Unocic, R. R. et al. Probing battery chemistry with liquid cell electron energy loss spectroscopy. *Chemical Communications*. **51** (91), 16377–16380 (2015).

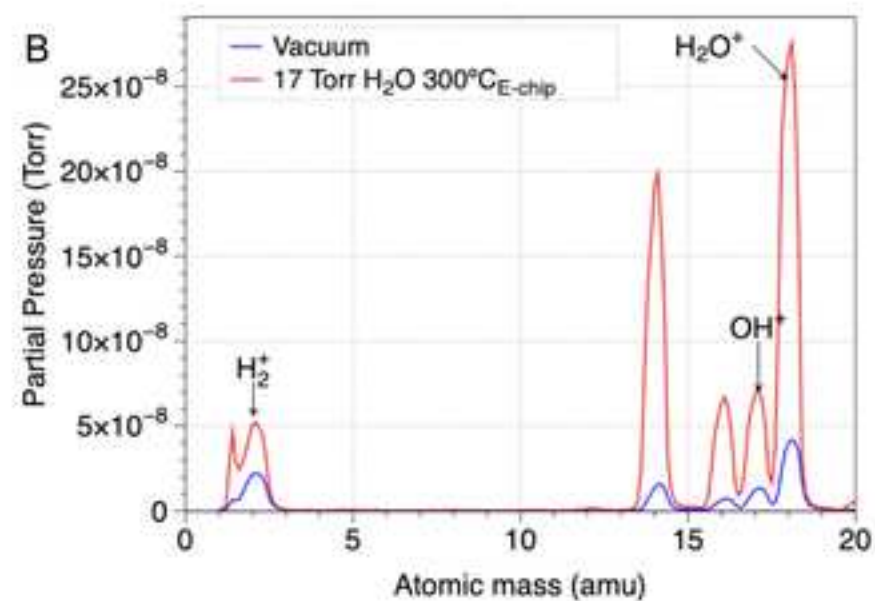
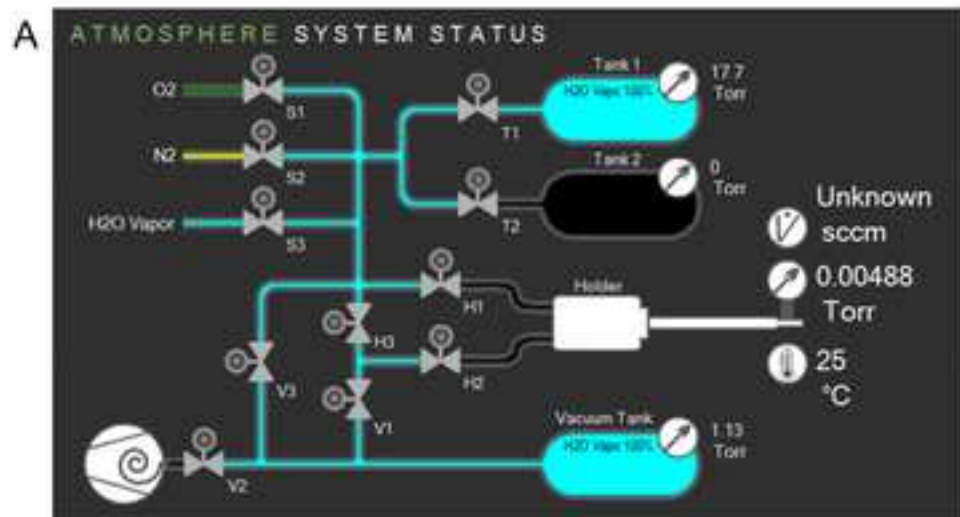


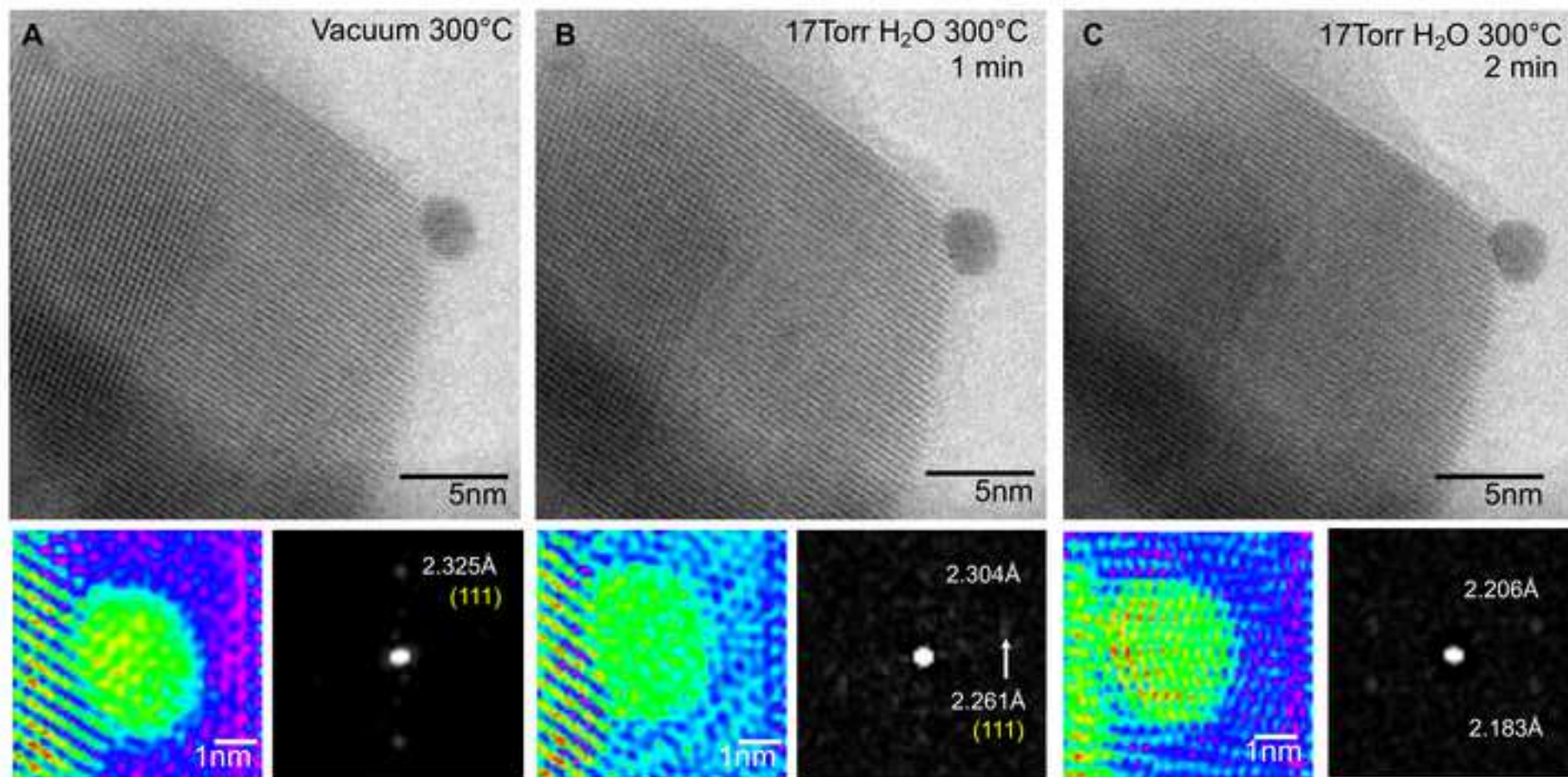


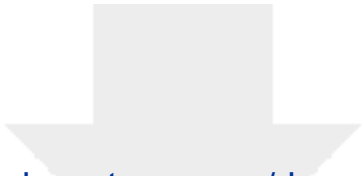




Note: Magenta color shows monitored system in 3A



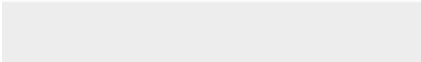




[Click here to access/download](#)

Table of Materials

Table of Materials_update.xlsx





PO Box 2008
Oak Ridge, TN 37831-6064
(865) 596-0996 | unocicka@ornl.gov

June 9th, 2021

Vineeta Bajaj, Ph.D.

Review Editor

JoVE

vineeta.bajaj@jove.com

Dear Dr. Bajaj,

Thank you very much for sending the reviewer comments and providing an opportunity for us to respond to the issues raised by the reviewers regarding our manuscript entitled, “Performing Closed-Cell Gas Reactions *In Situ* Electron Microscopy,” for publication in *JoVE Journal*. Our response to the reviewer’s comments and the changes we have made are outlined in the following section. Note that in our response, the original text/statements from the manuscript are shown in black, the corrections are shown in red, and responses are shown in blue. The highlighted in blue text refers to the new available audio files.

Sincerely,

Kinga A. Unocic

Research Staff Scientist

Materials Science and Technology Division

Oak Ridge National Laboratory

JoVE submission JoVE62174R2

Response to reviewer comments

Changes to be made by the Author(s) regarding the video:

1. Please increase the homogeneity between the video and the written manuscript. Ideally, all figures in the video would appear in the written manuscript and vice versa. The video and the written manuscript should be reflections of each other.

Response: [We believe that the video reflects the paper. We have a real video that shows the action and highlights the procedure in real time in more complete manner than shown in some figures.](#)

2. Furthermore, please revise the narration to be more homogenous with the written manuscript. Ideally, the narration is a word for word reading of the written protocol.

Response: [We originally had that done, but since then the Editor has requested additional changes to the manuscript; the movie was prepared by the ORNL production team, and our video expert has made numerous changes already. We cannot keep changing minor things, and our video expert has officially declined to address any further complicated edits. Our opinion is the following: we believe that any researchers who would be interested in and benefitted by this paper and the accompanying video are already expert microscopists, and only need help with the details \(protocol steps\) of the process, not e.g., how to load a sample into the electron microscope. Our protocol description is not \(and cannot be\) intended to train a novice microscopist to be able to complete a good in situ gas reaction experiment.](#)

3. Please ensure that the title of the submission is the same in the text and the manuscript.

Response: [We updated the title slide.](#)

4. Please ensure subheadings are the same in the text and the video.

Response: [We believe they match.](#)

5. Please ensure that there is a chapter title card: Representative results and it describes all the figures presented in the representative result section of the manuscript. The other figures can be shown wherever these are referenced in the text.

Response: [We added the "Representative results" card and the results are shown through the movie in real action.](#)

6. Please change the Summary card to Conclusion instead.

Response: [We kindly disagree with the comment, since this is a protocol, we believe that the title "Summary" is more suitable than "Conclusions".](#)

7. Please remove all the commercial terms from the video. e.g., protochips, atmosphere software, etc. Wherever possible please hide the commercial terms when showing the instrument.

Response: [Unfortunately, our ORNL production team will not be able to address this part.](#)

8. Please place the title card at the end of the video as well.

Response: [We placed the title card at the end of the video.](#)

9. • A lot are out of focus, at 3:44, 2:22, 2:48, 4:10, 5:32, 6:03, 8:33, 8:38, 9:50, 10:16

Response: [We kindly disagree with the Editor. This was done on purpose.](#)

10. • At 3:10 through 3:15 the video jumps between four different shots and figures too quickly for the viewer to grasp what is important

Response: [We believe it is just fine.](#)

11. • Voice over audio volume lowered significantly at 2:56

Response: We requested our production team to update it.
12. • When the speaker isn't talking, there is a clicking sound in the background. Please cut out the parts where the speaker isn't talking

Response: We believe the parts are needed for the coherency of the movie. Usually, it takes longer to show it.

Replay to Editor's comments:

1. In the video this is M-Bond, please change to cyanoacrylate glue as we cannot have commercial terms.

We requested that change to our ORNL team production.

2. In the video this is Preparation of Atmosphere holder. Please make it same in the video and the text. This part please ensure that the text and the narration is the same for this section and in the same order. Currently this does not match.

The small mismatch in wording is due to additional changes to the text of the manuscript that were requested by Editor, after the video was made. We cannot keep changing and updating the video → it is too time-consuming, and our ORNL production team has declined to keep doing it. We believe that the video is just fine as it is.

I did re-record the audio but our ORNL production team said they will not be able to work on this.

If we receive the raw file of the movie from ORNL production team, I can provide audio files to JoVE team to update the audio.

3. In the video please do not make a separate subheading “start the experiment” to make it homogenous with the text.

The “start the experiment card” was removed.

4. At 12:33 please insert a chapter title card in the video stating Representative results

We requested to add “Representative results” title card

5. Please ensure subsections headings are the same in the text and the video and follow the same order to make the manuscript text homogenous to the video.

We updated the order; I moved FIB section after Mask section.

6. As we are a methods journal, please ensure that the Discussion explicitly cover the following in detail in 3-6 paragraphs with citations:

- a) Critical steps within the protocol
- b) Any modifications and troubleshooting of the technique
- c) Any limitations of the technique
- d) The significance with respect to existing methods
- e) Any future applications of the technique

This was addressed as shown below:

“In the present work, an approach to perform *in situ* STEM reactions with and without water vapor is demonstrated. The critical step within the protocol is E-chip preparation and maintaining its integrity during the loading procedure. The limitation of the technique is (a) the specimen size and its geometry to fit the nominal 5- μm gap between paired (MEMS)-based silicon microchip devices as well as (b) a total pressure used in the experiments with water vapor since the highest total pressure depends on the quantity of water vapor. The significance of this method with respect to existing methods is that we can perform *operando* experiments, i.e., we analyze the specimens under real conditions, enabled by an RGA system that confirms/monitors experimental conditions. Additionally, there are opportunities for future applications of the technique to diverse materials systems that may require different methods and procedures for sample deposition on E-chip heaters.”